MODELING THE HYDRODYNAMICS OF A SPOUTING LAYER

P. V. Akulich, P. S. Kuts, and A. V. Akulich

UDC 533.6.011:66.096.5

We have developed a multizone hydrodynamic model of a conic spouting layer, consisting of averaged differential mass, momentum and angular momentum equations and accounting for the radial flow of the dispersed phase. We have obtained a numerical solution of the system of equations for the case in which the layer is divided into two zones, which is consistent with experimental data.

A spouting layer is efficient means of phase interaction, which has found its fairly wide application in many technological processes, in particular, the drying and thermal treatment of dispersed materials [1-4].

A prominent place in studying the spouting layer is occupied by the hydrodynamics of interacting phases, which determines the rate of heat and mass transfer processes and generally serves as a basis for their mathematical description. In connection with this, numerous investigations [1-12] are devoted to modeling the hydrodynamics of the spouting process. The following hydrodynamic models of flow structures of the dispersed phase in a spouting layer are known: that of ideal mixing, cellular, diffusional, and combined [1, 5-7]. Studies [1, 6, 8-11] rely on the methods of mechanics of interpenetrating continua, whose basis is formed by mass, momentum, and energy equations. Investigations are available [1, 12] that are based on a separate description of the phase motion applied mainly to the layer core which is characterized by a relatively low concentration of particles. The merits and demerits of the hydrodynamic models have to do with the choice and completeness of the realization of one or another approach to the modeling. In the familiar continual hydrodynamic models [1, 3, 8-11], two zones, differing markedly in the concentration of the dispersed phase, are, as a rule, discriminated: a spout core and a ring (a peripheral zone). The boundary of the zones is assumed known. The radial motion of the dispersed phase is here neglected.

Enhancement and optimization of the processes of heat and mass transfer in the spouting layer require a more in-depth investigation of all aspects of the layer hydrodynamics.

The current study has formulated a multizone continual model of the hydrodynamics of a conic spouting layer taking into account the flow of the dispersed phase between the zones along the layer height. A numerical solution is obtained for the system of equations when the layer is divided into two zones.

The following assumptions are made. A stationary case of the spouting process is considered. The layer is partitioned into n zones by conic surfaces with coordinates φ_i. The variation in the parameters along φ inside each zone is taken as linear. An axisymmetric motion of the phases is assumed. The effects related to an alteration of the interface are disregarded.

Using the system of equations for the motion of a heterogeneous mixture [13], we will write the following conservation equations in a spherical coordinate system. The mass equations are:

for the gas phase

$$\frac{1}{\varepsilon_i}\frac{d(v_{ri}\varepsilon_i)}{dr}+\frac{2v_{ri}}{r}-\frac{1}{r\beta}(v_{\varphi i}^{+}\sin\varphi_i-v_{\varphi i}^{-}\sin\varphi_{i-1})=0, \quad (1)$$

and for the dispersed phase

$$\frac{1}{1-\varepsilon_i}\frac{d[w_{ri}(1-\varepsilon_i)]}{dr}+\frac{2w_{ri}}{r}-\frac{1}{r\beta}(w_{\varphi i}^{+}\sin\varphi_i-w_{\varphi i}^{-}\sin\varphi_{i-1})=0. \quad (2)$$

Academic Scientific Complex "A. V. Lyukov Heat and Mass Transfer Institute, Belorussian Academy of Sciences,, Minsk. Translated from Inzhenerno-Fizicheskii Zhurnal, Vol. 64, No. 3, pp. 350-356, March, 1993. Original article submitted March, 31, 1992.

 1062-0125/93/6403-0284$12.50

The moment equations for the gas and dispersed phases are:

$$v_{ri}\frac{dv_{ri}}{dr}=\frac{\overline{v}_{\varphi i}^{2}}{r}-\frac{1}{\rho_g}\frac{dP_i}{dr}-\frac{n_i f_{ri}}{\varepsilon_i\rho_g}, \tag{3}$$

$$w_{ri}\frac{dw_{ri}}{dr}=\frac{\overline{w}_{\varphi i}^{2}}{r}-g\cos\frac{\varphi_{i-1}+\varphi_i}{2}+f_{\text{T}}g\sin\varphi_n+\frac{n_i f_{ri}}{\rho_{\text{M}}(1-\varepsilon_i)}. \tag{4}$$

The third term on the right side of Eq. (4), which is zero for all zones with i $\neq$ n and other than zero for the wall region (i = n), takes into account the force of particle friction against the chamber wall and the viscous force in the wall region.

The angular momentum equations for the gas and dispersed phases are:

$$v_{ri}\frac{d\overline{v}_{\varphi i}}{dr}+\frac{v_{ri}\overline{v}_{\varphi i}}{r}+\frac{1}{r\beta}(v_{\varphi i}^{+}\sin\varphi_i-v_{\varphi i}^{-}\sin\varphi_{i-1})\overline{v}_{\varphi i}-$$
$$-\frac{1}{r\beta}[(v_{\varphi i}^{+})^2\sin\varphi_i-(v_{\varphi i}^{-})^2\sin\varphi_{i-1}]=-\frac{(P_i^{-}-P_i^{+})\sin\varphi_i}{r\rho_g\beta}-\frac{n_i f_{\varphi i}}{\rho_g\varepsilon_i}, \tag{5}$$

$$w_{ri}\frac{d\overline{w}_{\varphi i}}{dr}+\frac{w_{ri}\overline{w}_{\varphi i}}{r}+\frac{1}{r\beta}(w_{\varphi i}^{+}\sin\varphi_i-w_{\varphi i}^{-}\sin\varphi_{i-1})\overline{w}_{\varphi i}-$$
$$-\frac{1}{r\beta}[(w_{\varphi i}^{+})^2\sin\varphi_i-(w_{\varphi i}^{-})^2\sin\varphi_{i-1}]=\frac{n_i f_{\varphi i}}{\rho_{\text{M}}(1-\varepsilon_i)}-g\varkappa\sin\frac{\varphi_{i-1}+\varphi_i}{2}, \tag{6}$$

where

$$n_i=\frac{6(1-\varepsilon_i)}{\pi d^3}; \tag{7}$$

$$\beta=\cos\varphi_i-\cos\varphi_{i-1}; \tag{8}$$

$$f_{ri}=\frac{1}{8}\pi d^2\rho_g\xi_i|\mathbf{v}_i-\mathbf{w}_i|(v_{ri}-w_{ri}); \tag{9}$$

$$f_{\varphi i}=\frac{1}{8}\pi d^2\rho_g\xi_i|\mathbf{v}_i-\mathbf{w}_i|(\overline{v}_{\varphi i}-\overline{w}_{\varphi i}). \tag{10}$$

The second term on the right side of Eq. (6) totally accounts for a normal component of the reaction force of the chamber wall and the dispersed phase to the isolated element.

We define the drag in the constrained flow conditions from the formula [13]

$$\xi_i=\frac{\varepsilon_i^2}{[1-1{,}16(1-\varepsilon_i)^{2/3}]^2}\xi_i^0(\text{Re}_i^*), \tag{11}$$

where

$$\text{Re}_i^*=\frac{\varepsilon_i}{1-1{,}16(1-\varepsilon_i)^{2/3}}\text{Re}_i; \tag{12}$$

$$\text{Re}_i=\frac{d\rho_{\text{r}}|\mathbf{v}_i-\mathbf{w}_i|}{\mu_g}; \tag{13}$$

$$|\mathbf{v}_i-\mathbf{w}_i|=\sqrt{(v_{ri}-w_{ri})^2+(\overline{v}_{\varphi i}-\overline{w}_{\varphi i})^2}. \tag{14}$$

To determine the drag $\xi^0_i(\text{Re}^*_i)$ appropriate to an unbounded gas flow past a single droplet, we resort to the correlation [14]

$$\xi_i^0(\text{Re}_i^*)=\frac{24}{\text{Re}_i^*}+0.248\left(1+\sqrt{1+\frac{194}{\text{Re}_i^*}}\right). \tag{15}$$

The parameters $v^-_{\varphi i}$, $v^+_{\varphi i}$, $w^-_{\varphi i}$, $w^+_{\varphi i}$, P^-_i, and P^+_i can be expressed in terms of $v_{\varphi i}$, $w_{\varphi i}$, P_i, and P_0 using the relations

$$\bar{v}_{\varphi i} = \frac{1}{2}(v^-_{\varphi i} + v^+_{\varphi i}),\ \bar{w}_{\varphi i} = \frac{1}{2}(w^-_{\varphi i} + w^+_{\varphi i}),\ \bar{P}_i = \frac{1}{2}(P^-_i + P^+_i). \tag{16}$$

The coupling conditions at the boundaries of the zones are written as follows:

$$v^+_{\varphi i} = v^-_{\varphi i+1}\frac{\varepsilon_{i+1}}{\varepsilon_i},\ w^+_{\varphi i} = w^-_{\varphi i+1}\frac{1-\varepsilon_{i+1}}{1-\varepsilon_i},\ P^+_i = P^-_{i+1}. \tag{17}$$

The boundary conditions for the system (1)-(16) are:

at the point of entry into the layer

$$\sum_{i=1}^{n}\varepsilon_i\rho_g v_{ri}F_{i0} = L_0,\ \sum_{i=1}^{m}(1-\varepsilon_i)w_{ri}F_{i0} = \sum_{i=m}^{n}(1-\varepsilon_i)w_{ri}F_{i0},$$
$$\bar{P}_i = P_{i0},\ \bar{v}_{\varphi i} = 0,\ \bar{w}_{\varphi i} = 0,\ \varepsilon_i = \varepsilon_{i0}, \tag{18}$$

and at the spout level

$$w_{ri} = 0.$$

From the condition that the side wall of the chamber is impermeable and the motion of phases is axisymmetric follows

$$\varphi = 0,\ v^-_{\varphi 1} = 0,\ w^-_{\varphi 1} = 0,\ \varphi = \varphi_n,\ v^+_{\varphi n} = 0,\ w^+_{\varphi n} = 0. \tag{19}$$

For simplicity we consider the case with the layer divided into two zones, viz., a spout core and a peripheral zone. Here relations (16) in view of Eq. (19) are written as

$$v^+_{\varphi 1} = 2\bar{v}_{\varphi 1},\ v^-_{\varphi 2} = 2\bar{v}_{\varphi 2},\ w^+_{\varphi 1} = 2\bar{w}_{\varphi 1};\ w^-_{\varphi 2} = 2\bar{w}_{\varphi 2},\ P^+_1 = 2\bar{P}_1 - P_0.$$

Then the system of equations for the spout core takes the form

$$\frac{dv_{r1}}{dr} + \frac{v_{r1}}{\varepsilon_1}\frac{d\varepsilon_1}{dr} + \frac{2}{r}(v_{r1} - \bar{v}_{\varphi 1}\gamma_1) = 0, \tag{20}$$

$$\frac{dw_{r1}}{dr} - \frac{w_{r1}}{1-\varepsilon_1}\frac{d\varepsilon_1}{dr} + \frac{2}{r}(w_{r1} - \bar{w}_{\varphi 1}\gamma_1) = 0, \tag{21}$$

$$v_{r1}\frac{dv_{r1}}{dr} = \frac{\bar{v}^2_{\varphi 1}}{r} - \frac{1}{\rho_g}\frac{d\bar{P}_1}{dr} - \frac{n_1 f_{r1}}{\varepsilon_1\rho_g}, \tag{22}$$

$$w_{r1}\frac{dw_{r1}}{dr} = \frac{\bar{w}^2_{\varphi 1}}{r} - g\cos\frac{\varphi_1}{2} + \frac{n_1 f_{r1}}{\rho_м(1-\varepsilon_1)}, \tag{23}$$

$$v_{r1}\frac{d\bar{v}_{\varphi 1}}{dr} + \frac{v_{r1}\bar{v}_{\varphi 1}}{r} - \frac{2\bar{v}^2_{\varphi 1}\gamma_1}{r} = -\frac{2(P_0 - \bar{P}_1)\gamma_1}{\rho_g r} - \frac{n_1 f_{\varphi 1}}{\rho_g\varepsilon_1}, \tag{24}$$

$$w_{r1}\frac{d\bar{w}_{\varphi 1}}{dr} + \frac{w_{r1}\bar{w}_{\varphi 1}}{r} - \frac{2\bar{w}^2_{\varphi 1}\gamma_1}{r} = \frac{n_1 f_{\varphi 1}}{\rho_м(1-\varepsilon_1)} - g\varkappa\sin\frac{\varphi_1 + \varphi_2}{2}, \tag{25}$$

where

$$\gamma_1 = \frac{\sin\varphi_1}{\cos\varphi_1 - 1}. \tag{26}$$

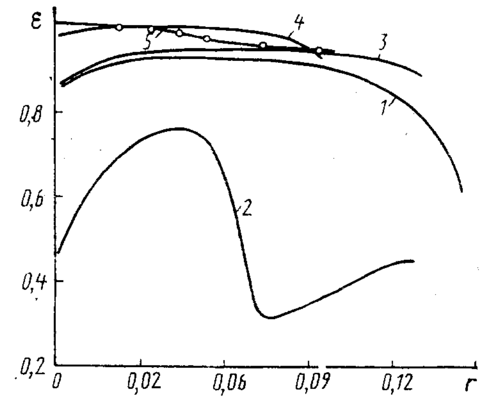

Fig. 1. Porosity distribution along the height of the spout core (curves 1, 3, 4, ϵ_1) and of the peripheral zone (curve 2, ϵ_2): 1, 2) v_{r0} = 11 m/sec, material is glass spheres; 3) 13; 4, 5) 34 m/sec, silica gel, computed and experimental relations, respectively [15]. r, m.

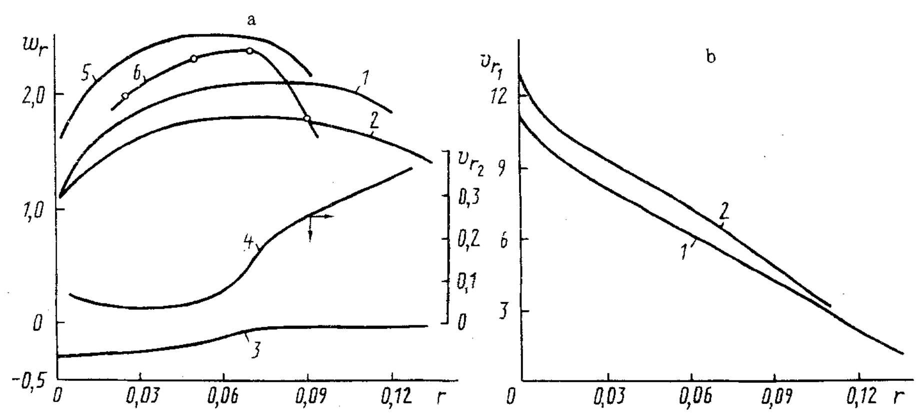

Fig. 2. Variation in the vertical velocity component of the gas and liquid along the layer height in the spout core and the peripheral zone: a, 1) w_{r1}, v_{r0} = 13 m/sec, material is glass spheres; 2) w_{r1}; 3) w_{r2}; 4) v_{r2} at v_{r0} = 34 m/sec, silica gel, computed and experimental [15] relations, respectively; b, 1, 2) v_{r1}, material is glass spheres; 1) v_{r0} = 11 m/sec; 2) 13. w_r, v_{r1}, m/sec.

For the peripheral zone, Eqs. (1)-(3) are similar to Eqs. (20)-(22), with the only difference that

$$\gamma_2 = \frac{\sin\varphi_1}{\cos\varphi_1 - \cos\varphi_2}. \tag{27}$$

Equation (4) rearranges to the form

$$w_{r2}\frac{dw_{r2}}{dr} = \frac{\overline{w}_{\varphi 2}^2}{r} - g\cos\frac{\varphi_1+\varphi_2}{2} + \frac{n_2 f_{r2}}{\rho_{\text{M}}(1-\varepsilon_2)} + g f_{\text{fr}}\sin\varphi_2. \tag{28}$$

In conformity with Eq. (17), instead of Eqs. (5) and (6) we use the relationships

$$\overline{v}_{\varphi 2} = \overline{v}_{\varphi 1}\frac{\varepsilon_1}{\varepsilon_2}, \quad \overline{w}_{\varphi 2} = \overline{w}_{\varphi 1}\frac{1-\varepsilon_1}{1-\varepsilon_2}. \tag{29}$$

Analogously to [9], for closing the boundary conditions (18) in the numerical solution the systems of equations were varied by the value of the velocity v_{r1} at the point of entry into the layer. The pressure difference $P_1 - P_0$ was

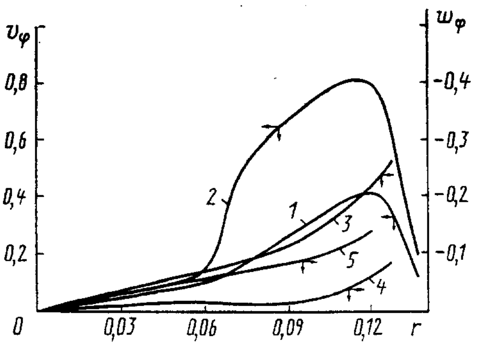

Fig. 3

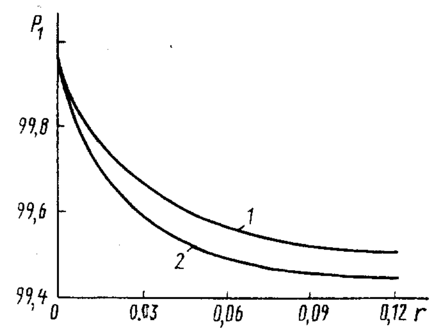

Fig. 4

Fig. 3. Variation in the radial velocity component of the gas and particles along the layer height: 1) $v_{\varphi 1}$; 2) $v_{\varphi 2}$; 3) $w_{\varphi 1}$; 4) $w_{\varphi 2}$ at v_{r0} = 11 m/sec; 5) $w_{\varphi 1}$, r_{r0} = 13 m/sec. v_{φ}, $_w\varphi$, m/sec.

Fig. 4. Pressure distribution along the spout height: 1) v_{r0} = 11 m/sec; 2) 13. P_1, kPa.

approximated by a piecewise linear function that was determined experimentally. The system of equations (20)-(29) with the closing relations (7)-(15) and the boundary conditions (18) was solved numerically by the Runge-Kutta method of fourth order.

The computations have been performed for two conic-type devices. In the first, with the diameter of inlet opening D = 0.032 m, the angle of taper $\theta = 40°$, and the initial height of the layer H = 0.12 m, glass spheres of diameter d = 10^{-3} m and density ρ = 2500 kg/m^3 were subject to spouting. In the second, with D = 0.015 m, $\theta = 45°$, and H = 0.1 m, the layer is formed by silica gel particles with d = $4 \cdot 10^{-3}$ m and density ρ_M = 1120 kg/m^3 (Figs. 1 and 2). In accordance with [1], the angle of the spouting core was taken to be 6°.

It is evident from the computed vertical profiles of the layer porosity (Fig. 1) that the core porosity in the middle of the layer depends slightly on the height, and afterwards its appreciable decrease is observed, corresponding in practice to the formation of a densified "cap" of the spout. An increase in the gas flow rate diminishes the particle concentration in the spout. The porosity of the peripheral zone in the layer bottom rises abruptly, remaining smaller than the core porosity, i.e., a larger expansion occurs due to the conic geometry of the device. Further on, the porosity decreases to about a value of $\epsilon_2 = 0.4$, corresponding to a loose packing of the layer. As might be expected, the relations for the vertical velocity component of the gas and the particles in the layer, given in Fig. 2, indicate a rise in the particle velocity in the region of the spout mouth and its fall at the top of the layer. The vertical velocity component v_{r1} of the gas in the spout core decreases with height, whereas the gas velocity v_r in the peripheral zone increases, which results from the enhancement of the radial gas flow from the spout core (Fig. 3). Here, the gas flow to the periphery decreases sharply at the layer level owing to equalization of the pressure in the core and peripheral zone in the upper part of the spout. It follows from the relations presented in Fig. 3 that the radial velocity of the dispersed phase flow in the peripheral zone, directed to the device axis, depends weakly on the vertical coordinate, except for the layer top, where its increase is observed, whereas the radial velocity in the spout increases more intensely. Therefore, the radial flow of the dispersed phase increases with the layer height, therewith a rise in the inlet velocity of the gas causing it to decline slightly. The relations for variation in the gas pressure in the spout core, given in Fig. 4, point to the fact that the pressure fall is the greatest in the spout bottom, which is due to the interaction of the high-velocity gas flow with the low-mobile layer of particles. Obviously, an increase in the gas flow rate leads to the pressure decrease.

It is seen from Figs. 1 and 2 that the computations for the spouting of silica gel particles presented for the porosity and the velocity of particles in the spout core are in favorable agreement with experimental data [15].

The hydrodynamic model suggested can be used to design and optimize spouting-layer devices.

NOTATION

d, equivalent diameter of the particles, m; D, diameter of the inlet opening of the device, m; F, cross-sectional area of the layer, m^2; f_{fr}, coefficient taking into account the force of particle friction against the device wall and the viscous force of the particles, $f_{fr} = 2.4\text{-}2.6$ was taken; g, acceleration by gravity, m/sec^2; H, initial height of the layer, m; L, mass flow rate of the gas, kg/sec; P, gas pressure, Pa; P_0, gas pressure on the device axis, Pa; r, φ, coordinates of the spherical system; v, w, velocities of the gas and dispersed phases, m/sec; θ, angle of taper of the device, deg; $\varkappa$, coefficient equal to $\varkappa = 1\text{-}2.2$; ϵ, layer porosity; μ_r, dynamic viscosity of the gas, Pa·sec; ρ_r, ρ_M, gas and particle pressure, kg/m^3.

Subscripts: i, zone number, $1 \leq i \leq n$, r, φ, projection on the coordinate axis; m, zone number pertaining to the boundary of the spout core; 0, value at the point of entry into the layer; $-$, $+$, values at the inner and outer boundaries of the zone, respectively; $-$, average over the cross section; 1, 2, values corresponding to the spout core and the peripheral zone.

LITERATURE CITED

1. K. Matur and N. Epstein, Spouting Layer [Russian translation], Leningrad (1978).
2. P. G. Romankov and N. B. Rashkovskaya, Drying in Suspension [in Russian], 3rd edition, Leningrad (1979).
3. V. F. Frolov, Modeling of Drying of Dispersed Materials [in Russian], Leningrad (1987).
4. A. E. Gorshtein, "Scientific principles of improving the technology of ultramarine and other inorganic substances using a spouting layer," Engineering Sciences Doctor Dissertation, Leningrad (1983).
5. U. Mann and E. J. Crosby, Ind. Chem. PDD., **11**, 314-318 (1972).
6. V. E. Babenko, A. A. Oigenblik, and É. M. Zhiganova, Teor. Osn. Khim. Tekhnol., **11**, No. 5, 728-735 (1975).
7. V. V. Shectopalov, V. V. Men'shikov, and V. V. Kafarov, Khim. Neft. Mashinostr., No. 6, 14-15 (1978).
8. V. V. Kafarov, I. N. Dorokhov, and É. M. Kol'tsova, Systematic Analysis of the Processes of Chemical Engineering [in Russian], Moscow (1988).
9. V. V. Kafarov, I. N. Dorokhov, É. M. Kol'tsova, and N. V. Men'shutina, Teor. Osn. Khim. Tekhnol., **20**, No. 1, 44-50 (1986).
10. L. M. Galieva and Yu. P. Gupalo. Teor. Osn. Khim. Tekhnol., **23**, 449-454 (1989).
11. Yu. V. Vasil'yev and V. F. Frolov, Zh. Prikl. Khim., **57**, No. 2, 314-319 (1984).
12. V. E. Kutsakova, L. I. Logimov, and S. F. Demidov, Zh. Prikl. Khim., **11**, No. 11, 2519-2524 (1979).
13. R. I. Nigmatulin, Dynamics of Multiphase Media [in Russian], Part 1, Moscow (1987).
14. M. É. Aérov and O. M. Todes, Hydraulic and Thermal Bases of Operation of Devices with Stationary and Boiling Granular Layer [in Russian], Leningrad (1968).
15. V. D. Mikhailik, N. V. Antonishin, et al., Izv. AN BSSR, Ser. Fiz.-Tékh. Navuk, No. 3, 81-86 (1967).